J Membrane Biol (2011) 240:121–129
DOI 10.1007/s00232-011-9350-1

ORIGINAL ARTICLES

Direct or Indirect Regulation of Calcium-Activated Chloride Channel by Calcium

Yafei Chen · Hailong An · Ting Li · Yani Liu · Chongsen Gao · Peng Guo · Hailin Zhang · Yong Zhan

Received: 10 January 2011 / Accepted: 14 February 2011 / Published online: 19 March 2011

Abstract Calcium-activated chloride channels (CaCCs) play fundamental roles in numerous physiological processes. Despite their physiological importance, the molecular identity of CaCCs has not been fully investigated until now. Recently, transmembrane 16A (TMEM16A) was demonstrated by three independent research groups to be a strong candidate for the CaCC molecular basis. To further investigate the electrophysiological characteristics, we constructed TMEM16A (abcd) stably transfected HEK293 cell lines and carried out whole-cell and excised inside–out patch-clamp experiments. The TMEM16A channel was Ca^{2+}-dependent in both patch configurations. The TMEM16A current could be strongly inhibited by niflumic acid, and when Cl^- was substituted by gluconate ions, the current was reduced considerably. In inside–out configuration, TMEM16A channel was time-independent but voltage-dependent, in which the half-maximum activating free Ca^{2+} concentration was 63 nM at 80 mV. While in whole-cell configuration, the current was both time- and voltage-dependent. About the rectification feature, the TMEM16A current also showed distinct characteristics in the two patch configurations. In whole cells, the TMEM16A channel expressed outward rectification at low Ca^{2+} concentration but when the Ca^{2+} concentration was high it became linear. On the contrary, in inside–out configuration, it always expressed outward rectification. Comparing the different characteristics in the two configurations, some underlying mechanisms remain to be identified, which is discussed with respect to direct or indirect activation. There was irreversible rundown in this channel.

Keywords Calcium-activated chloride channel · Activation characteristic · Transmembrane protein 16A (TMEM16A) · Rectification · Electrophysiology · Pharmacology

Y. Chen · H. An · T. Li · C. Gao · P. Guo · Y. Zhan (✉)
School of Sciences, Hebei University of Technology, Tianjin 300130, China
e-mail: zhany@hebut.edu.cn; cyf800205@yahoo.com.cn

Y. Liu · H. Zhang
Department of Pharmacology, Hebei Medical University, Shijiazhuang 050017, China

Introduction

Calcium-activated chloride channels (CaCCs) were first described in the 1980s in *Xenopus* oocytes (Barish 1983), where they were activated by increasing Ca^{2+} concentration upon fertilization to prevent polyspermy. Now, it has been found that CaCCs play several important roles in many cells from various types of neurons to epithelium, cardiac muscle and smooth muscle. They participate in many vital biological processes, including cell volume regulation, neuronal and cardiac excitability, smooth muscle contraction and transendothelial ion/fluid transport (Eggermont 2004; Hartzell et al. 2005; Galietta 2009).

Although the current of CaCCs (also written as $I_{Cl.Ca}$) has been studied for nearly 30 years, its molecular identity is still a matter of controversy; it is very important in understanding how they work in normal physiological or pathological processes. Several candidate proteins, CLCA, CLC-3, bestrophines and Tweety, have been nominated; but they express different electrophysiological characteristics from typical CaCCs (Galietta 2009). Actually, the hallmark CaCC feature is the unique voltage dependence modulated by different intercellular Ca^{2+} concentrations.

At nonmaximal Ca^{2+} concentrations, CaCCs are activated by positive membrane potential and deactivated by negative membrane potential, therefore showing outwardly rectifying current–voltage relationships. At maximal Ca^{2+} concentrations, however, CaCCs are fully activated at all membrane potentials, showing a linear current–voltage relationship. Such properties do not fully fit any of the above-mentioned candidates (Schroeder et al. 2008). Recently, three independent groups identified that TMEM16A is a strong candidate for CaCCs (Yang et al. 2008; Schroeder et al. 2008; Caputo et al. 2008); they used different experimental and bioinformational methods to obtain nearly the same results, indicating the credibility of the conclusion. However, questions on this point have remained, until now. There are questions about whether TMEM16A is an independent channel protein or acts as part of a more complex transporting macromolecule (Galietta 2009; Hartzell et al. 2009).

To further explore these questions, we stably transfected TMEM16A(abcd) in HEK293 cells and adopted two patch-clamp recording modes, excised inside–out patch and whole-cell, to further examine in detail its electrophysiological characteristics at different Ca^{2+} concentrations and in conditions in which Ca^{2+} was substituted by other anions and in the presence of a chloride channel inhibitor.

We found that the TMEM16A channel was Ca^{2+}-dependent in both patch configurations. It could be strongly inhibited by niflumic acid (NFA), and when the chloride ions were substituted by gluconate ions, the current was also reduced considerably. With respect to the rectification feature, we obtained distinct results in the two configurations. In whole-cell, the TMEM16A channel expressed outward rectification at low Ca^{2+} concentration; but at high Ca^{2+} concentration, it became linear. On the contrary, in inside–out, it always expressed outward rectification. Comparing the different characteristics in the two configurations, we proposed that direct or indirect activation might be the reason for the different time dependence and rectification features. There was irreversible rundown in excised inside–out configurations.

Materials and Methods

Chemicals

All cell culture reagents and Lipofectamine 2000 were purchased from Invitrogen (Carlsbad, CA). HEPES, $MgCl_2{\cdot}6H_2O$, NFA, EGTA, gluconate sodium salt and 1 M standard $CaCl_2$ solution were purchased from Sigma (St. Louis, MO). Other chemical reagents were purchased from Chinese companies.

Cell Culture and Stable Transfection

The human cDNA clone hANO1, also called TMEM16A(abcd), was kindly provided by Prof. Young Duk Yang (Seoul National University, Seoul, Korea) and subcloned to expression vector pEGFPN1 (Clontech, Palo Alto, CA). HEK293 cells were maintained in DMEM with 10% fetal bovine serum, 100 UI/ml penicillin and 100 μg/ml streptomycin and passaged about three times a week. Stable transfection of pETMEM16A to HEK293 cells was performed as described by Jia et al. (2007) with Lipofectamine 2000. Stably transfected HEK293 cells were seeded in 24-well plates on 12-mm glass coverslips 1 day before patch recording. All cells were cultured in an incubator with 5% CO_2 at 37°C.

Solutions

For whole-cell recordings, the pipette solutions contained (in mM) CsCl 130, EGTA 10, $MgCl_2{\cdot}6H_2O$ 1, HEPES 10 and MgATP 1, adjusted to pH 7.3 with CsOH with added standard $CaCl_2$ (1 M, Sigma) to various free Ca^{2+} concentrations (calculated according to http://www.stanford.edu/~cpatton/CaEGTA-NIST.htm). Total Ca^{2+} concentrations were 0 for nominal, final concentration 5.27 mM 1 M standard $CaCl_2$ solution for 100 nM free Ca^{2+}, 8.69 mM for 600 nM, adjusted to pH 7.3 with CsOH. The perfusion solution contained (in mM) NaCl 150, $CaCl_2$ 1, $MgCl_2{\cdot}6H_2O$, glucose 10, mannitol 10 and HEPES 10, adjusted to pH 7.4 with NaOH.

For inside–out recordings, the pipette solution contained (in mM) NaCl 130, $MgCl_2{\cdot}6H_2O$, HEPES 10 and MgATP 1, adjusted to pH 7.3 with CsOH. The perfusion solution contained (in mM) NaCl 140, $MgCl_2{\cdot}6H_2O$, HEPES 10 and EGTA 5, adjusted to pH 7.4 with NaOH, and added 1 M standard $CaCl_2$ solution to various free Ca^{2+} concentrations calculated with the software (see Web site above). Added total Ca^{2+} concentrations were 0 for nominal, final concentration 1.30 mM 1 M standard $CaCl_2$ solution for 20 nM free Ca^{2+}, 3.18 mM for 100 nM, 4.57 mM for 600 nM, 4.73 mM for 1,000 nM and 4.98 mM for 10,000 nM.

NFA was dissolved in dimethyl sulfoxide (DMSO) as a 100-mM stock solution and diluted to 2 mM in perfusion solution in inside–out recordings.

When the channel's special permeability to Cl^- was assayed, the bath solutions (BSs) contained (in mM)

BS1: NaCl 130, $MgCl_2{\cdot}6H_2O$, HEPES 10, EGTA 5
BS2: NaCl 130, $MgCl_2{\cdot}6H_2O$, HEPES 10, $CaCl_2$ 0.1
BS3: Na-gluconate 130, $MgCl_2{\cdot}6H_2O$, HEPES 10, EGTA 5
BS4: Na-gluconate 130, $MgCl_2 \cdot 6H_2O$, HEPES 10, $CaCl_2$ 0.1

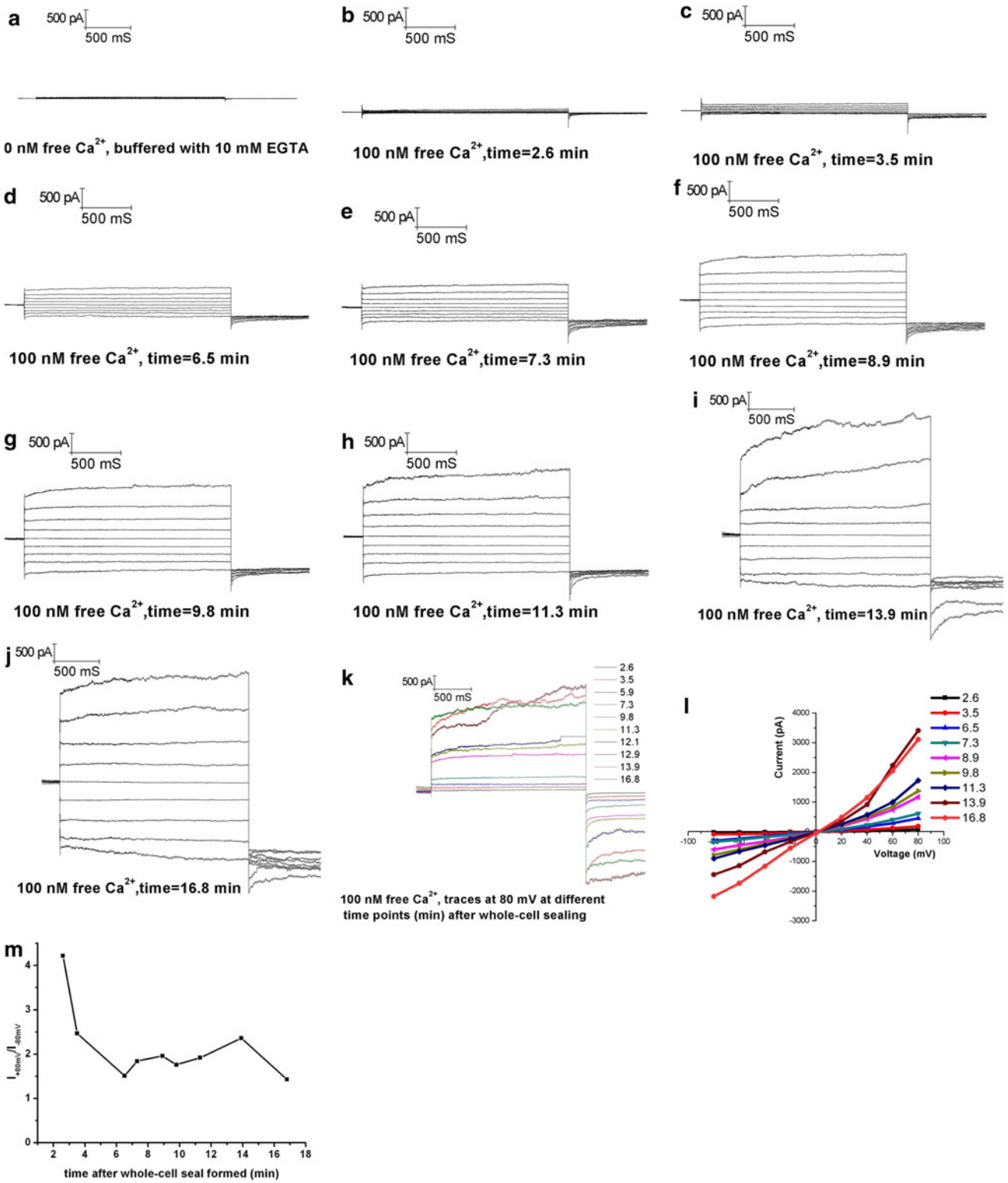

Fig. 1 Representative whole-cell recordings of Ca^{2+} and time dependence of the TMEM16A channel when the pipette solutions contained 0 and 100 nM free Ca^{2+}. **a** Activation currents: The pipette solution contained nominal 0 Ca^{2+}, buffered with 10 mM EGTA. **b–j** Activation currents at different time points after the whole-cell seal formed, with pipette solutions containing 100 nM free Ca^{2+}. **k** Current traces at 80 mV at different time points (min) after the whole-cell seal formed. **l** Current–voltage relationship activated by 100 nM Ca^{2+} measured at the end of the voltage steps from the cell shown in (**b–k**). **m** Quantitative description of outward description at 100 nM Ca^{2+}, ratio of I_{80} to I_{-80} at different time points after whole-cell formed in **l**

Electrophysiology

Electrophysiological recordings from TMEM16A stably transfected HEK293 cells were performed in whole-cell or inside–out patch-clamp configuration. Patch pipettes were made of borosilicate glass (Bona, China) with a P-97 puller (Sutter Instruments, Novato, CA) and fire-polished to 600–800 KΩ (inside–out mode) or 2–4 MΩ (whole-cell mode) resistance, respectively.

Data were acquired with an EPC-10 amplifier controlled by Pulse software with Digi LIH1600 interface (Heka, Lambrecht/Pfalz, Germany). Data were low-pass-filtered at 2.9 kHz and sampled at 3.33 kHz. All measurements were performed at room temperature. Graphics and statistical data analysis were carried out with Origin 8.0 (OriginLab, Northampton, MA).

Results

Ca^{2+} Dependence and Rectification Characteristics of Stable-State Activation Currents Study Using Whole-Cell Configuration

Using the TMEM16A stably transfected HEK293 cells, whole-cell recordings were performed with different Ca^{2+} concentrations, which was diffused from pipettes to whole-cell sealing cells. The stimulus protocol is shown in Fig. 3a.

We observed that when the pipette solution contained nominal 0 Ca^{2+} (trace Ca^{2+} in the solution was chelated with 10 mM EGTA), the whole-cell currents remained at several tens of picoamperes (Fig. 1a), nearly negligible throughout over 20 min of continuous recording ($n = 10$).

Figure 1b–j shows activation currents of a representative cell in the presence of 100 nM free Ca^{2+} in the pipette solution over time. When the whole-cell seal had just begun (time = 2.6 and 3.5 min, respectively; Fig. 1b, c), currents were like those in 0 Ca^{2+} condition because Ca^{2+} had not diffused into the cell or had not yet sufficiently activated the TMEM16A channel in those short time segments. At 6.5 min (Fig. 1d), the current increased significantly, to nearly 500 pA; and as time passed, the currents increased to about 3.5 nA by 17 min. Similar results were obtained in seven cells, and the mean activation time was 6.0 ± 1.5 min. We describe as "activation" when the current reaches several hundreds of picoamperes and shows obvious time-dependent activation at 60 and/or 80 mV. The activation current traces at 80 mV at different time points are plotted in Fig. 1k. To investigate the rectification characteristics, current–voltage curves at different time points after whole-cell sealing formed are summarized in Fig. 1l. After activation of the channel, it showed outward rectification in early phase (0–11 min, Fig. 1l); however, it showed a mild but significant linear trend in the end (17 min, Fig. 1l). Figure 1m is a quantitative description of the TMEM16A current rectification feature, which was indicated by the ratio of I_{80mV} to I_{-80mV}. When the ratio was near 1, the rectification was defined as linear; and we defined it as more outward rectification the more it increased beyond 1. It could be seen that the outward rectification was sustained over the whole recording time.

Fig. 2 Representative whole-cell recordings of Ca^{2+} and time dependence of the TMEM16A channel when the pipette solutions contained 600 nM free Ca^{2+}. **a–k** Activation currents at different time points after the whole-cell seal formed. **l** Current traces at 80 mV change at different time points (min) after the whole-cell seal formed. **m** Current–voltage relationships activated by 600 nM Ca^{2+} measured at the end of the activation voltage steps from the cell shown in (**a–l**). **n** Quantitative description of outward description at 600 nM Ca^{2+}, ratio of I_{80} to I_{-80} at different time points after whole-cell formed in (**m**). **o** Activation currents with 2 mM NFA and 1,000 nM Ca^{2+} in pipette solution

When it came to 600 nM free Ca^{2+} in the pipette solution, activation of the TMEM16A channel became faster than that at 100 nM free Ca^{2+}. At 0.7 min after the seal formed, the current showed obvious time-dependent activation (Fig. 2a, b). The current developed to considerably activate in nearly 2 min, and it increased quickly to the maximum value in about 6 min (Fig. 2c–k). We obtained similar results in six cells, and the mean activation time was 2.5 ± 0.5 min. The activation current traces at 80 mV at different time points are plotted in Fig. 2l. The current–voltage curves at different time points after the whole-cell seal formed are summarized in Fig. 2m. After activation of the TMEM16A channel, it began to show outward rectification (0–8 min, Fig. 2m), but at the end of full activation at 600 nM Ca^{2+} concentration, it became significantly linear (9–11 min, Fig. 2n). Finally, the current response to a high concentration of 2 mM NFA together with 1,000 nM Ca^{2+} in the pipette solution was tested (Fig. 2o, $n = 8$). The current became very small (about 60 pA) but still showed a significant time-dependent feature and strong inhibition of NFA, which demonstrated that it was a chloride channel. The quantitative description of outward rectification is shown in Fig. 2n. It can be seen that in the first 8 min after the whole-cell seal formed, the feature was outward rectification but that at the end of recording it became linear.

Ca^{2+} Dependence and Rectification Characteristics of Stable-State Activation Currents Using Excised Inside–Out Patches

To further investigate Ca^{2+} activation of the TMEM16A channel, more flexible control of Ca^{2+} concentrations in

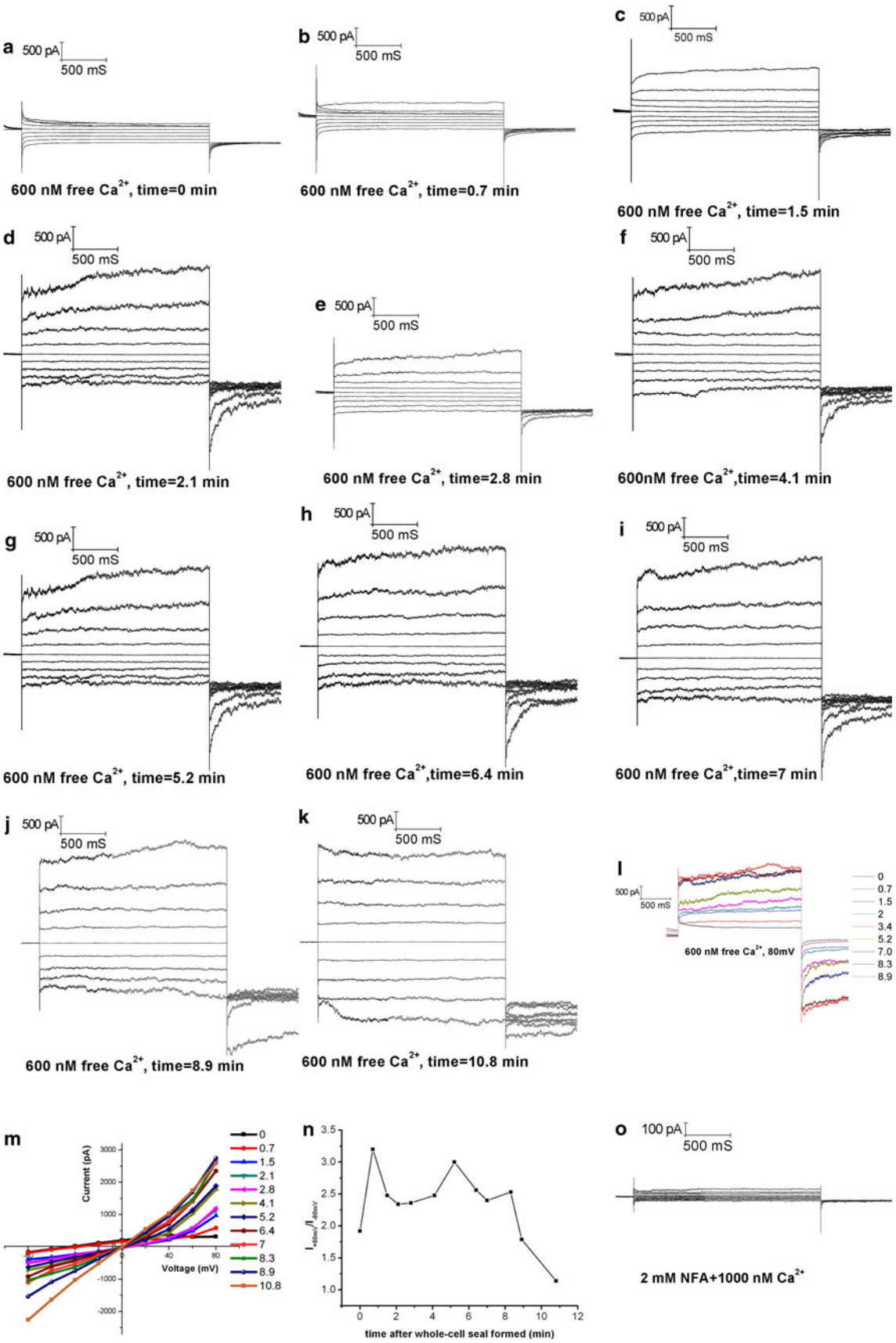
a
500 pA
500 mS
600 nM free Ca2+, time=0 min
b
500 pA
500 mS
600 nM free Ca2+, time=0.7 min
c
500 pA
500 mS
600 nM free Ca2+, time=1.5 min
d
500 pA
500 mS
600 nM free Ca2+, time=2.1 min
e
500 pA
500 mS
600 nM free Ca2+, time=2.8 min
f
500 pA
500 mS
600nM free Ca2+,time=4.1 min
g
500 pA
500 mS
600 nM free Ca2+, time=5.2 min
h
500 pA
500 mS
600 nM free Ca2+,time=6.4 min
i
500 pA
500 mS
600 nM free Ca2+,time=7 min
j
500 pA
500 mS
600 nM free Ca2+, time=8.9 min
k
500 pA
500 mS
600 nM free Ca2+, time=10.8 min
l
500 pA
500 mS
600 nM free Ca2+, 80mV
0
0.7
1.5
2
3.4
5.2
7.0
8.3
8.9
m
Current (pA)
Voltage (mV)
0
0.7
1.5
2.1
2.8
4.1
5.2
6.4
7
8.3
8.9
10.8
n
time after whole-cell seal formed (min)
o
100 pA
500 mS
2 mM NFA+1000 nM Ca2+

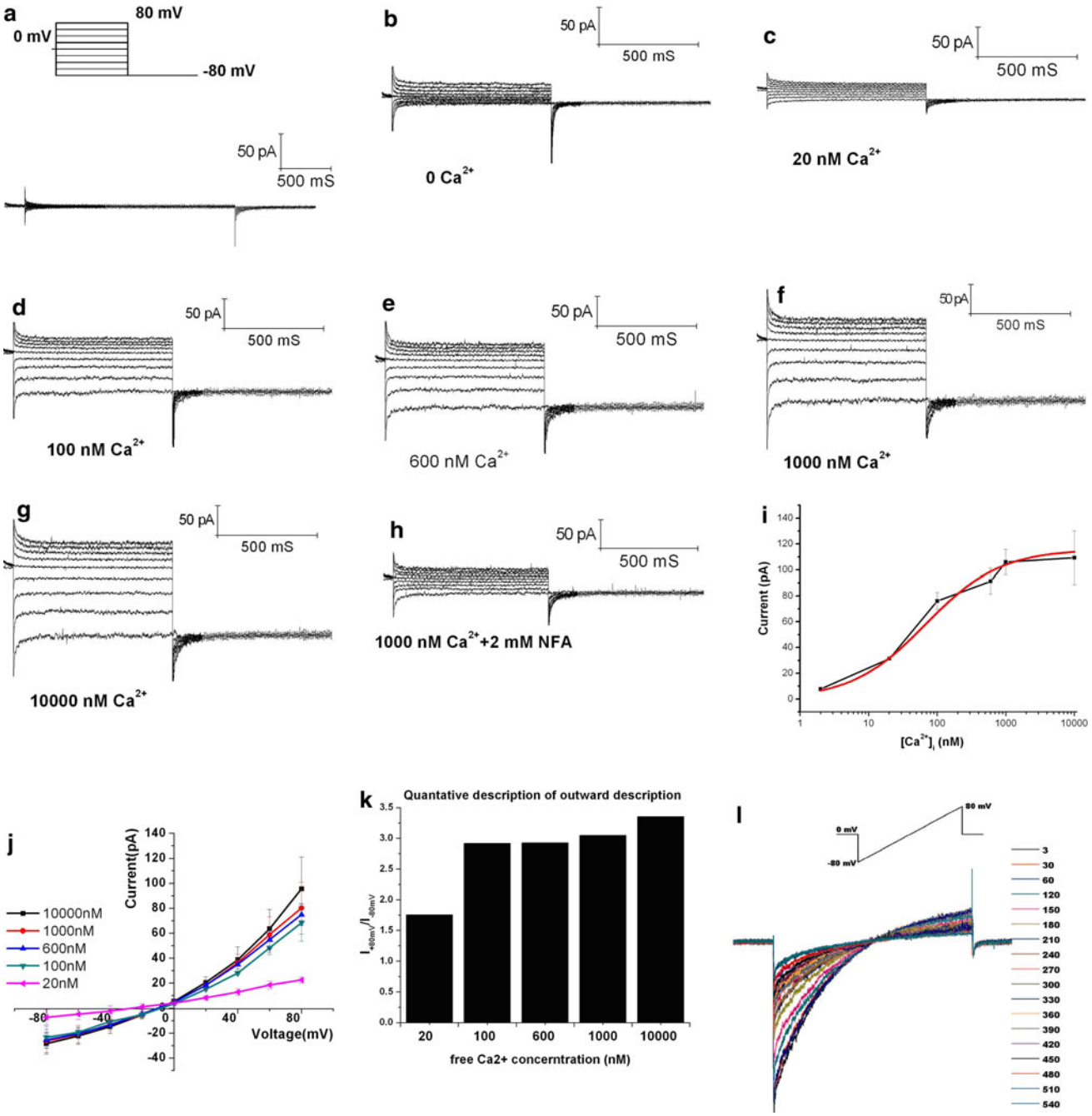

Fig. 3 Activation of various concentrations of Ca^{2+} to TMEM16A and inhibition of NFA in excised inside–out configuration. **a** Stimulus waveform and activation current in untransfected HEK293 cells. **b–h** Increasing activation currents at different concentrations of Ca^{2+} (in nM) and inhibition of 2 mM NFA. **i** Dose–response curve in inside–out patch; data points were fitted to the Hill equation. **j** Current–voltage relationships at the end of the activation voltage steps at various Ca^{2+} concentration activation currents. Error bars, mean ± SEM. **k** Ratio of mean value of currents at 80 and −80 mV, quantitative description of the outward rectification at different Ca^{2+} concentrations. **l** Rundown with 600 nM free Ca^{2+} both in pipette and bath solutions

excised inside–out configuration was carried out with the HEK293 cells. In these experiments, a homemade perfusion system was adopted to ensure about 1 min/ml solution change. In these experiments, the excised membrane patch was held in front of a glass pipette, and various concentrations of Ca^{2+} were applied to the adjacent place of the pipette.

Figure 3a shows that there were no endogenous TMEM16A currents in untransfected HEK293 cells ($n > 30$). Figure 3b–g shows activation currents by

exposing the cytoplasmic side of the patches to various concentrations of Ca^{2+}. The dose–response curve of TMEM16A to Ca^{2+} is plotted in Fig. 3i, and the half-maximum activating Ca^{2+} concentration was 63 nM. It can be seen that as Ca^{2+} concentrations increased, the currents grew larger but that when the concentrations were higher than 600 nM, the amplitude of activation currents seemed to stop augmenting. To investigate whether the channel was a special Cl^- transporter, the TMEM16A channel response to NFA was examined, and we observed that 2 mM NFA could inhibit 80% of the activation currents, as shown in Fig. 3h. Similar results were obtained from five patches. The rectification feature in the inside–out mode is also shown in Fig. 3j; the *I–V* curves always showed significant outward rectification as the concentration of Ca^{2+} increased to the maximum value. The quantitative description of the rectification is shown in Fig. 3k. It can also be seen that the outward rectification always increased significantly with increasing Ca^{2+} concentration. Evident rundown phenomenon was recorded in most inside–out patches, as shown in Fig. 3l; and this rundown was irreversible.

The Ca^{2+}-Activated Current Is Carried Out by Cl^-

To investigate whether the Ca^{2+}-activated current observed in excised inside–out patches was really a Cl^- current, the activation/tail currents and the reversal potential changes when Cl^- was replaced by gluconate ions were measured. The solutions have been described in "Materials and Methods" section.

In Fig. 4, we see that in solution BS1 (containing 10 nM free Ca^{2+}) the maximum activation/tail currents were small but increased to 130 pA when the perfusion solution was changed to BS2 (containing 0.1 mM Ca^{2+}), which indicates the activation response of TMEM16A to Ca^{2+}. However, when the Cl^- was substituted by gluconate ions (BS3 and BS4), the maximum activation/tail currents both reduced to 65 pA, whether in the presence or the absence of 0.1 mM Ca^{2+}, demonstrating the TMEM16A currents were mainly permeable to Cl^-, not gluconate ions. The current–voltage relationship is shown in Fig. 4c. Compared to the evident outward rectification in BS2 solution containing 0.1 mM Ca^{2+}, currents recorded from gluconate ions containing BS3 and BS4 solutions showed obvious inward rectification. The reversal potential also changed with replacement of Cl^- with gluconate ions, as indicated in Fig. 4d.

Discussion

Our results support the idea that TMEM16A may be the molecular basis of CaCCs, although it cannot be excluded that TMEM16A needs to assemble with other proteins yet to be identified to form the CaCC.

The TMEM16A channel is Ca^{2+}-dependent. In whole-cell configuration, the beginning activation time in 600 nM

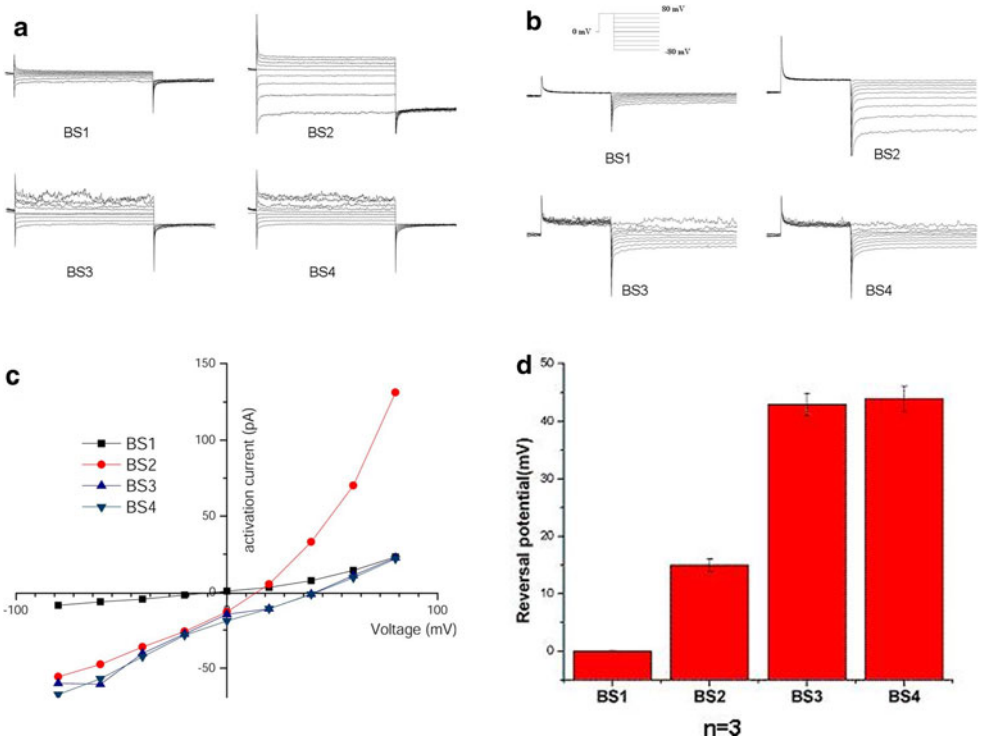

Fig. 4 Anion selectivity of TMEM16A channel. **a**, **b** Activation and tail currents in different perfusion solutions: BS1 containing nominal 0 Ca^{2+} (buffered with 5 mM EGTA) and 130 mM Cl^-, BS2 containing 0.1 mM Ca^{2+} and 130 mM Cl^-, BS3 containing nominal 0 Ca^{2+} and 130 mM gluconate, BS4 containing 0.1 mM Ca^{2+} and 130 mM gluconate. **c** Current–voltage relationships summarized at the end of the activation voltage steps in (**a**). **d** Reversal potential changes with different solutions in (**c**)

free Ca^{2+} was shorter than that in 100 nM free Ca^{2+}, due to the more powerful diffusing gradient of Ca^{2+}. In excised inside–out configuration, the half-maximum activating Ca^{2+} concentration was 63 nM at 80 mV, smaller than that in the previous report (Yang et al. 2008), in which it was 400 nM at 60 mV in ANO1-ET_AR (endothelin receptor subtype A)–transfected HEK293 cells. The reason might mainly lie in that we activated the TMEM16A channel directly by Ca^{2+}, while in the Yang et al. (2008) report, the channel was activated indirectly by ET_AR, a more complex signal-transduction pathway involving more cytosolic components and, thus, less sensitivity.

The TMEM16A channel could be strongly inhibited by NFA (a chloride channel inhibitor) in both patch configurations, and when Cl^- was substituted by gluconate ions, the current also reduced considerably. These results were consistent with Yang et al. (2008) and Schroeder et al. (2008). Thus, it could be concluded that this TMEM16A was surely a CaCC.

There are still controversies about the mechanism through which Ca^{2+} activates the TMEM16A channel. It has been reported that the CaCC was activated indirectly through calmodulin (Kaneko et al. 2006), by means of Ca^{2+}-dependent phosphorylation (Xie et al. 1996), or directly by Ca^{2+} in another CaCC candidate molecular counterpart, TMEM16B (Pifferi et al. 2009). In this study, the time dependence in the two patch configurations was compared. In whole-cell, the TMEM16A current was time-dependent, taking 500 mS or longer to develop to maximal values (Figs. 1, 2), consistent with Caputo et al. (2008). On the contrary, in excised inside–out configuration, the TMEM16A current was time-independent, no obvious increase being seen at any specific depolarized voltages. By comparing these results, it could be deduced that in inside–out configuration the TMEM16A channel was directly activated by Ca^{2+} but in whole-cell the channel was activated by more complex, and currently unknown, mechanisms in the cytoplasm, due to the prolonged activation time.

About the rectification feature, distinct results in the two patch configurations were obtained. In whole-cell, when Ca^{2+} in pipette solution had just begun to diffuse into cells (the Ca^{2+} concentration was low), the TMEM16A channel expressed obvious outward rectification; but when the Ca^{2+} concentration was high, the rectification feature became linear. These results were consistent with the review by Galietta (2009). However, it was found that in inside–out configuration it always expressed outward rectification, which was different from the current report. One plausible explanation is that in whole-cell the TMEM16A channel could be fully activated, so it could transport the maximum currents at both 80 and −80 mV. In excised inside–out configuration, however, without any cytosolic components on the cytoplasmic side, the TMEM16A channel was not fully activated, so it transported a larger current at 80 mV than at −80 mV. This question is very interesting and requires further investigation. In summary, we raised the hypothesis that full activation (perhaps involving both direct and indirect activation) required multiple signal-transduction reactions and produced maximum activation currents at both depolarized and polarized voltages, while partial activation (possibly involving only direct activation) required only Ca^{2+} and produced maximum activation only at depolarized voltage.

There was irreversible rundown in excised inside–out configuration, indicating that some unknown modulatory components of the TMEM16A channel may be lost after excision of the membrane (Reisert et al. 2005)

Because of the diversity of CaCC types and sources, there are many open questions about the electrophysiological character of CaCC and the newly discovered molecular counterpart TMEM16A. This report provides detailed patch-clamp records in both whole-cell and inside–out configurations and raises one hypothesis of full (perhaps both direct and indirect) or partial (maybe only direct) activation of Ca^{2+} to TMEM16A. Further investigation is needed to enrich our knowledge about the CaCC activation and inhibition processes, and this could be the foundation of further pathological and pharmacological research in related diseases.

Acknowledgements We thank Dr. Jia Zhanfeng and Dr. Zhang Xuan for their help and discussion on experimental technology. This study was supported by Grants from the National Natural Science Foundation of China (10975045, 10775038) and the Natural Science Foundation of Hebei Province (C2009000029).

References

Barish ME (1983) A transient calcium-dependent chloride current in the immature *Xenopus* oocyte. J Physiol 342:309–325

Caputo A, Caci E, Ferrera L et al (2008) TMEM16A, a membrane protein associated with calcium-dependent chloride channel activity. Science 322:590–594

Eggermont J (2004) Calcium-activated chloride channels: (un)known, (un)loved? Proc Am Thorac Soc 1:22–27

Galietta LJV (2009) The TMEM16 protein family: a new class of chloride channels? Biophys J 97:3047–3053

Hartzell C, Putzier I, Arreola J (2005) Calcium-activated chloride channels. Annu Rev Physiol 67:719–758

Hartzell HC, Yu K, Xiao Q et al (2009) Anoctamin/TMEM16 family members are Ca^{2+}-activated Cl^- channels. J Physiol 587: 2127–2139

Jia QZ, Jia ZF, Zhao ZY et al (2007) Activation of epidermal growth factor receptor inhibits KCNQ2/3 current through two distinct pathways: membrane PtdIns(4, 5)P2 hydrolysis and channel phosphorylation. J Neurosci 27:2503–2512

Kaneko H, Mohrlen F, Frings S (2006) Calmodulin contributes to gating control in olfactory calcium-activated chloride channels. J Gen Physiol 127:737–748

Pifferi S, Dibattista M, Menini A (2009) TMEM16B induces chloride currents activated by calcium in mammalian cells. Pflugers Arch 458:1023–1038

Reisert J, Lai J, Yau KW et al (2005) Mechanism of the excitatory Cl^- response in mouse olfactory receptor neurons. Neuron 45:553–561

Schroeder BC, Cheng T, Jan YN et al (2008) Expression cloning of TMEM16A as a calcium-activated chloride channel subunit. Cell 134:1019–1029

Xie W, Kaetzel MA, Bruzik KS et al (1996) Inositol 3,4,5,6-tetrakisphosphate inhibits the calmodulin-dependent protein kinase II–activated chloride conductance in T84 colonic epithelial cells. J Biol Chem 271:14092–14097

Yang YD, Cho H, Koo JY et al (2008) TMEM16A confers receptor-activated calcium-dependent chloride conductance. Nature 455:1210–1215